Journal of Physical and Theoretical Chemistry
of Islamic Azad University of Iran, 13 (1) 25-34: Spring 2016
(J. Phys. Theor. Chem. IAU Iran)
ISSN 1735-2126

Theoretical Structural and Spectral Analyses of TEMPO Radical Derivatives of Fullerene

Fatih Ucun*, Serkan Kaya and Halil Oturak

Department of Physics, Faculty of Arts and Sciences, Süleyman Demirel University, 32260 Isparta, Turkey

Received April 2016; Accepted May 2016

ABSTRACT

The spectroscopic properties of the 2,2,6,6-tetramethyl-piperidine-1-oxyl (TEMPO) radical derivatives of the fullerene (C_{60}) were theoretically investigated. The ground state optimized structures of the radical adducts of the fullerene were calculated by using DFT (B3LYP) with 6-31 G(d) level. It was concluded that a 6-6 ring junction of C_{60} moiety generally covalently links to the piperidine ring of the TEMPO derivatives, directly. The optimization characteristics of all the fullerene radical derivatives indicate generally a annulene structure while C_{60}+TEMPO indicate a cyclopropane structure which is formed by the link of the carbon of the piperidine ring doubly to a 6-6 ring junction of C_{60}. The calculated isotropic hyperfine coupling constants, vibrational frequencies and UV- Vis transition energies of all the radical adducts were seen to be in good agreement with the corresponding experimental data. The UV-Vis transitions and their energies were determined with corresponding to the experimental values. In the IR analysis the shifts of vibrational frequencies have been commented by comparison with those belonged to the pure C_{60}. Also the some selected geometrical parameters with together the cage width and the cage length for the ground state optimized structures of all the radical adducts were listed, and the binding energies of the radicals were obtained.

Keywords: Fullerene; TEMPO; DFT; Radical; Spectral Analysis

INTRODUCTION

The introduction of spin labels into the fullerene molecules transforms them into objects convenient for Electron Paramagnetic Resonance (EPR) studies. A variety of labels designed to be observed by spectroscopic techniques including fluorescence, optical absorption, EPR and i.e. is known for probing local environment, molecular rotational motion, and bioorganic structure. Nitroxide free radicals have been introduced as spin label in a variety of molecular structures for studying their structural and dynamic properties [1,2]. Although nitroxide radicals do not affect the electronic distribution of the labeled molecule in the ground state and in the excited states the populating and decay pathways and decay rates of the excited states are strongly affected by the presence of the extra spin, through small interactions with other electron spins. All the neutral species of typical nitroxide radicals give EPR spectra consisting of a main triplet of lines with about 15 G splitting by the ^{14}N

*Corresponding author: fatihucun@sdu.edu.tr

nucleus. A spin-labeled reagent fullerene (2,2,6,6- tetramethyl – piperidine – 1 - oxyl) [C_{60}(TEMPO)] is synthesized and, characterized by spectroscopic, magnetic and electrochemical measurements by lshida and et al. [3]. The same authors also pyrolyzed the sodium salt of 4-oxo-TEMPO tosylhydrazone in chlorobenzene in the presence of C_{60} to obtain the adducts $C_{60}(TEMPO)_n$ (n = 1 – 3) and, characterized them by mass, Infrared (IR), UV(Ultraviolet) and EPR spectroscopies [4]. In the present work, the optimized structures of the 2,2,6,6-tetramethyl-piperidine -1-oxyl (TEMPO) radical derivatives of the fullerene (C_{60}) have been calculated by using density-functional theory (DFT) based Beck-3 Lee Young Parr (B3LYP) functional WITH 6-31+G(D,p) basis set. Their spectral (EPR, IR, UV-Visible) analysis have been performed, and some structural properties were determined.

COMPUTATIONAL DETAILS

All the calculations were performed using Gaussian 09 Rev. D.01 Intel Xeon SC 3.40 GHz cpu package [5] and Gauss-View molecular visualization programs [6] on the personal computer. The structures were optimized by using spin-uNRESTRICTED DFT (B3LYP) method with 6-31G(d) basis set. The calculations of λ_{max}'s in the UV-Vis spectra corresponding to the vertical excitation energies were carried out by using TD-DFT method with the B3LYP functional and the same 6-31G(d) basis set selected for the geometry optimization. For the TD-DFT calculations the Polarizable Continuum Model (PCM) was used to take care of the solvent effects [7, 8], and dichloro-methane solution was chosen. The calculated vibrational frequencies were scaled with a scale factor of 0.9614 for the DFT (B3LYP) 6-31G (d) level [9]. The assignments of all the fundamental vibrational modes were obtained by means of the potential energy distribution (PED) analysis using VEDA 4 program [10]. The binding energies of the labeled radicals were calculated using supramolecular approach corrected for basis set superposition error (BSSE) according to Boys counterpoise method [11] at the optimized level.

RESULTS AND DISCUSSIONS

Optimized structures

The calculated ground state optimized structures of all the C_{60}(TEMPO) radical adducts are shown in Fig. 1. Both the 6-6 and 6-5 ring fusions of C_{60} to a TEMPO derivative were separately taken and the more stable one with lower energy were chosen. As known the fullerene C_{60} consisting of sixty carbon atoms has a cage-like carbon cluster. All the atoms are chemically equivalent, and only two kinds of carbon- carbon bonds are present on its molecular structure. The C–C, C=C bond lengths and cage width of C_{60} in the solid phase are experimentally obtained as 1.46, 1.40 and, 7 $\mathring{A}$ [12, 13], respectively, and we have calculated these as 1.464, 1.385 and 7.114 $\mathring{A}$ at DFT (B3LYP) 6-31 G(d) level, respectively. C_{60} shows no distortion from a spherical shape with the distance of individual atoms. But, the bond lengths and cage width are considerably altered comparing to those in the bound radicals. The some selected geometrical parameters (bond length, cage width and cage length) for all the radical products are given in Table 1. The separation of spherical shape of the C_{60} (TEMPO) products can easily be understood from the values in the table. The used TEMPO radical derivatives of the fullerene (C_{60}) in this study are as follows:

UV-Vis transitions

In the pure TEMPO the N–O group is responsible for the absorption in both the

UV and visible regions. Moreover, this group is described as having a half anti-bonding π* bond by 1 e^- as exemplified in Fig. 2. The π and π* orbitals are generated from the combination of the nitrogen lone pair and the $2p_y$ and $2p_z$ orbitals of the oxygen. The energy levels and some possible transitions are shown in the figure. The orbital forms of the highest singly occupied.

molecular orbital [SOMO (π *)] and lowest unoccupied molecular orbital [LUMO(σ*)] and the other orbitals can also be seen in the figure. Relatively nonbonding energy levels at intermediate energies can be particularly difficult to rank in energy. Proficiency at estimating orbital energies is only gained by experience, and by always attempting to correlate molecular orbitals and their energies with experimental properties of the molecules under consideration [14]. Essentially, the energy of a nonbonding orbital is that of an atomic orbital and, is typically in between the energy of a bonding orbital and the energy of an anti-bonding orbital.

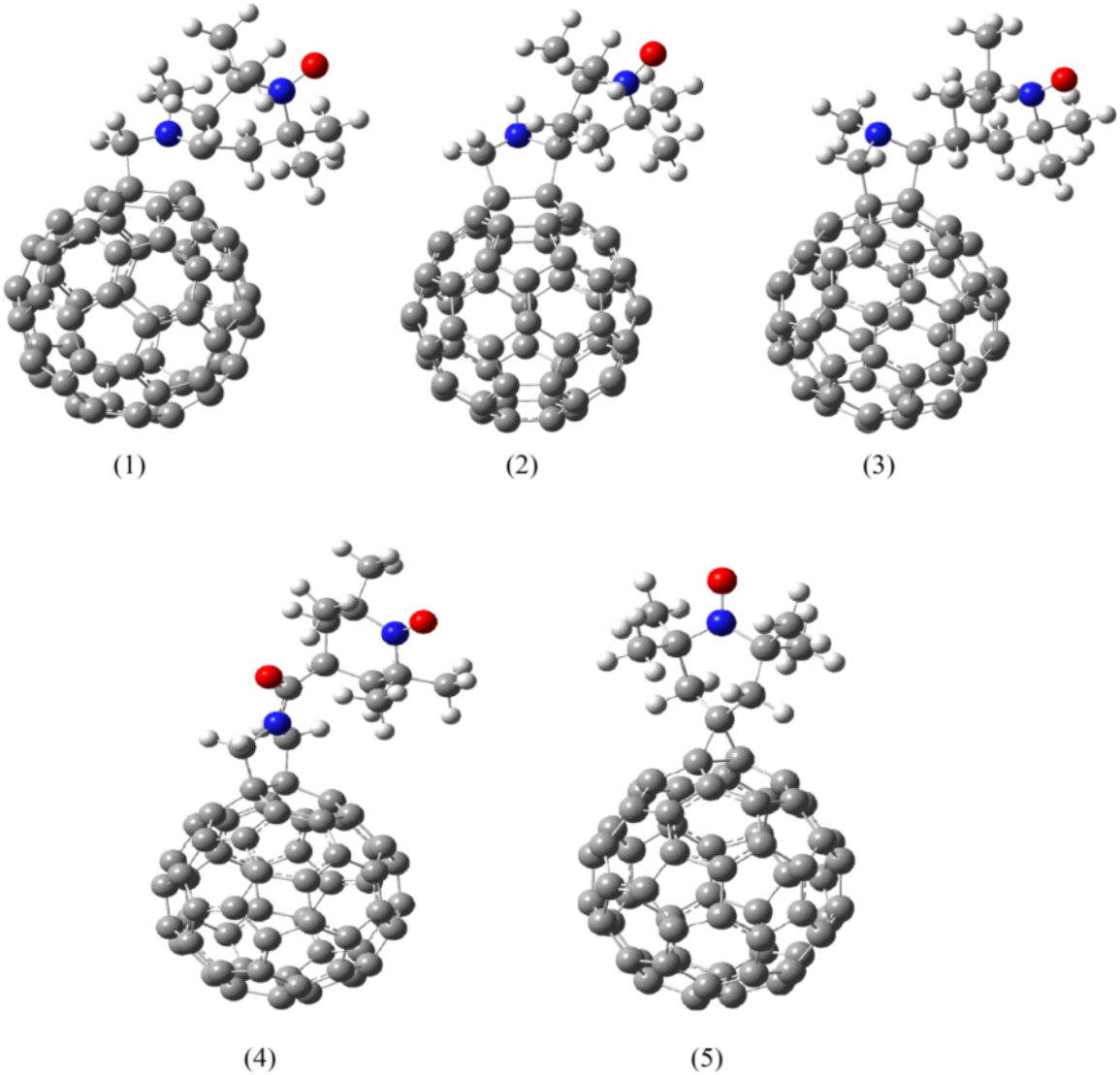

Fig. 1. The optimized molecular structures of the 2,2,6,6-tetramethyl-piperidine-1-oxyl radical derivatives of the fullerene.

Table 1. The some selected bond lengths, cage lengths and cage widths of the C_{60} (TEMPO) radical products calculated at DFT (B3LYP) 6-31G (d). The experimental values for C_{60} are given in parenthesis

Bond Length ($\overset{o}{A}$)	C_{60}	(1)	(2)	(3)	(4)	(5)
C-C	1.464 (1.460)	1.453	1.453	1.453	1.454	1.454
C=C	1.364 (1.400)	1.397	1.396	1.396	1.396	1.396
C=O	-	-	-	-	1.228	-
N-O	-	1.285	1.283	1.285	1.286	1.283
$C\text{-}CH_3$	-	1.541 1.543	1.540 1.545	1.538 1.544	1.539 1.544	1.538 1.543
$N\text{-}CH_3$	-	1.454	-	1.463	-	-
Cage Length	7.114 (7.000)	7.471	7.463	7.449	7.428	7.341
Cage Width	7.114 (7.000)	7.111	7.113	7.112	7.116	7.111
C-C fusion	-	1.616	1.621	1.611	1.614	1.618

Values in parenthesis taken from [12, 13].

(1) *N-Methyl-3,4-fulleropyrrolidine-2-spiro-4′-(2′,2′,6′,6′-tetramethylpiperidine-1′-oxy)*
(2) *3,4-Fulleropyrrolidine-2-spiro-4′-(2′,2′,6′,6′-tetramethylpiperidine-1′-oxyl)*
(3) *N-Methyl-3,4-fulleropyrrolidine-2-spiro-4′-(2′,2′,6′,6′-tetramethylpiperidine-1′-oxyl)*
(4) *N-[(2′,2′,6′,6′-tetramethylpiperidinyl-1′-oxyl)carbonyl]-3,4-fulleropyrrolidine*
(5) *C60 +Tempo (the carbon of the pyrrolidine ring doubly linked to a ring junction of C60).*

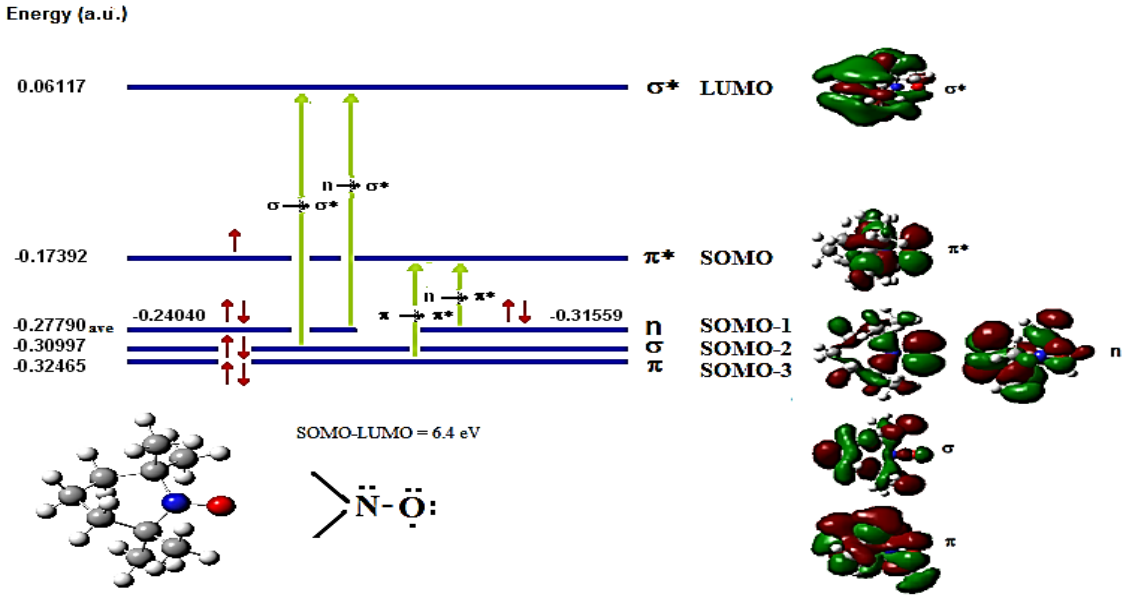

Fig. 2. The molecular energy levels, some possible UV-Vis transitions and orbital forms for the 2,2,6,6-tetramethyl-piperidine-1-oxyl.

So, we have used the average energy of the two non-bonding orbitals with electrons to obtain a good value corresponding experimental one. The

experimental energy value of n → π* transition for TEMPO is 425-478 nm [15] in different solutions, and its calculated value is439 nm.

In the pure C_{60} the energies of Huckel molecular π orbitals and their symmetries are given in Fig. 3 by the help of Haddon's calculations [16]. The energies of the highest occupied molecular orbital (HOMO) and lowest unoccupied molecular orbital (LUMO) are the main orbital taking part in chemical reaction, which are very important characteristics of the fullerene C_{60}. As seen from the figure the HOMO (h_u) and LUMO (t_{1u}) orbitals are five-fold and three-fold degenerated, respectively. The energy difference between the HOMO and LUMO orbitals is 1.9 eV. The optically permitted gap of the fullerene h_u-t_{1g} is 2.9 eV. At the ground state the degrees of degeneracy of LUMO+1(t_{1g}), LUMO + 2 (t_{2u}+h_g), HOMO-1(g_g) HOMO-2(h_g) HOMO-3(h_g+t_{1u}+a_g) orbitals are 3, 8, 4, 5, and 9, respectively. The possible transitions and their energies corresponding to the experimental values [17] (in parenthesis) are given in Fig. 3.

In Table 2 are seen some possible UV-Vis transitions and their energies with together the HOMO and LUMO energy gap for all the radical products of C_{60}. The experimental values in the table are obtained from Ref. [17] and, given in the parenthesis. As seen the UV-Vis transition energies for all the derivative products are only slightly shifted to longer or shorter wavelengths as compared to the experimental values. From the table we can also see that the radical derivative products (1)-(4) of C_{60} exhibit experimental observable bands between 216- 430 nm while its radical derivative (5) gives also two Vis peaks at around 540 and 600 nm but not a band at around 430 nm. From their calculated optimized structures in Fig. 1 we attributed this to their different links to the TEMPO radical derivatives. So we state that the radical derivative products (1)-(4) of C_{60} have a 6-6 annulene structure while C_{60}+TEMPO has a 6-6 cyclopropane structure. For a better understanding the possible transitions and their energies corresponding to the experimental values for the radical derivatives (1) and (5) of C_{60} are given in Figs. 4 and 5 with together the SOMO and LUMO orbitals, respectively. As seen the LUMO orbitals of the radical derivatives (1) and (5) are totally localized on the fullerene cage while their SOMO orbitals are totally and partially localized on the TEMPO derivative, respectively. This may be attributed to have their different annulane-like structures.

From Table 2 we can also understand that the SOMO and LUMO energy levels and the SOMO–LUMO gap (*ΔE*) is heavily dependent on the labeled radical. The smaller gap between the SOMO and LUMO orbitals characterizes their lower molecular chemical stability [18]. As seen, the SOMO–LUMO gap for the radical derivative (4) of C_{60} is lowest while it is highest for its radical derivatives (1) and (3).

The calculated maximum absorption values (λ_{max}) and oscillator strengths (f) in the UV-Vis spectra are 807 nm 0, 808 nm 0, 1002 nm $62x10^{-4}$, 808 nm 0 and 778 nm 0 for the radical derivatives (1)-(5), respectively.

IR absorption spectra

The calculated IR absorption spectra of all the C_{60}(TEMPO) radical products with together those belonged to the pure C_{60} and TEMPO are given in Fig. 6. In the figure the experimental vibrational frequency values are given in the parenthesis [17,19,20]. The calculated vibrational frequencies in the figure are scaled, and their assignments are obtained by means of the potential energy distribution (PED)

analysis using VEDA 4 program [10]. The four characteristic bands of C_{60} is 1429, 1182, 575, and 526 cm^{-1} [19]. These bands belong to stretching, bending, torsion and out of plane bending modes, respectively. Our calculated values at DFT(B3LYP) 6-31 G(d) level are 1465, 1136, 560, 510 cm^{-1}, respectively. As understand from the calculated IR spectra of the derivative products of C_{60} in Fig. 6 the stretching and bending modes shift to longer wavelengths as around 10 cm^{-1} and 50 cm^{-1}, respectively, while the torsion and out of plane bending modes stay nearly same as compared to those of the pure fullerene. The C_{60} bands become weaker in the spectra of its derivative products. Also, the addition of radical to the fullerene C_{60} brings a lowering of the symmetry of the resulting compound and, gives rise to a number of bands assigned to the bending vibrations.

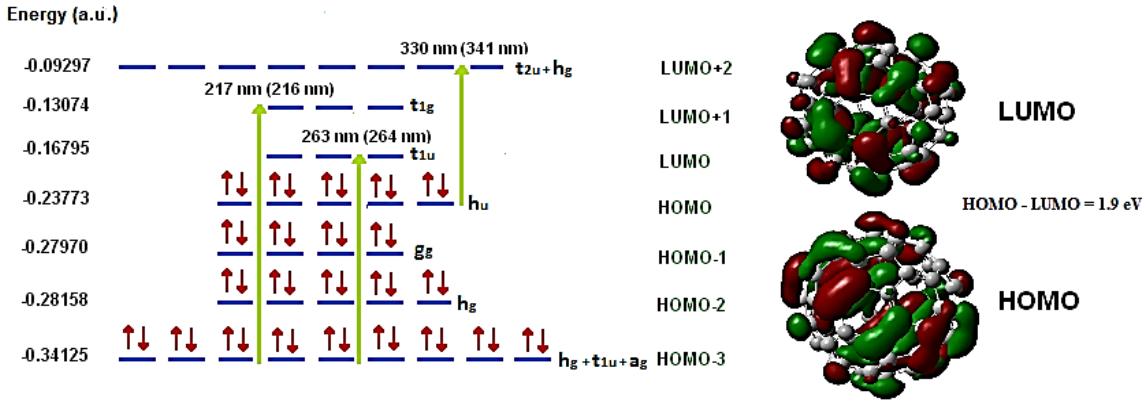

Fig. 3. The Huckel molecular π orbitals, symmetries and some possible UV-Vis transitions for the fullerene with together some orbital forms. The experimental UV-Vis transitions are given in parenthesis [17].

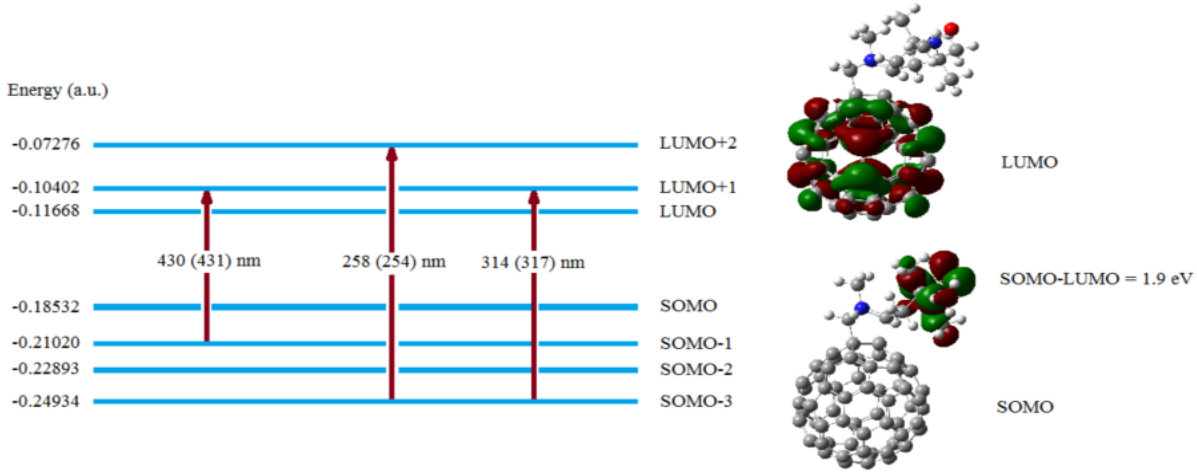

Fig. 4. The molecular energy levels, some possible UV-Vis transitions and orbital forms for the radical derivative (1) of the fullerene. The experimental UV-Vis transition energies are given in parenthesis [17].

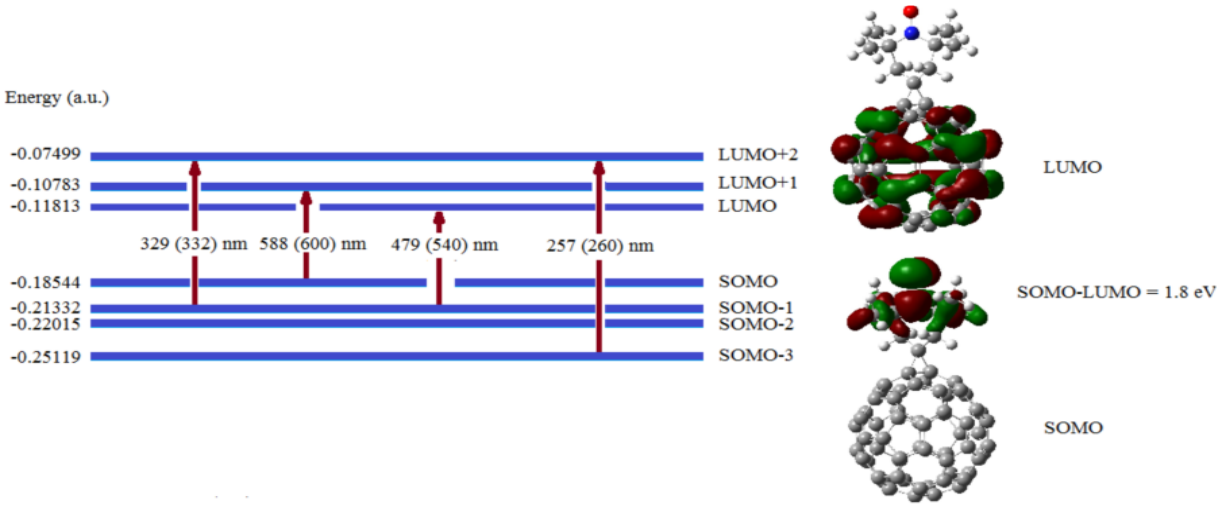

Fig. 5. The molecular energy levels, some possible UV-Vis transitions and orbital forms for the radical derivative (5) of the fullerene. The experimental UV-Vis transition energies are given in parenthesis [17].

Table 2. The UV-Vis transitions and energies for the C_{60} (TEMPO) radical products with together the HOMO and LUMO energy gap. The experimental values are given in parenthesis

C_{60}	HOMO-3→LUMO+1	217 nm (216 nm)
	HOMO-3→LUMO	264 nm (264 nm)
	HOMO→LUMO+1	316 nm (341 nm)
	HOMO-LUMO	1.9 eV
(1)	SOMO-3→LUMO+2	258 nm (254 nm)
	SOMO-3→LUMO+1	314 nm (317 nm)
	SOMO-1→LUMO+1	430 nm (431 nm)
	SOMO-LUMO	1.9 eV
(2)	SOMO-3→LUMO+2	267 nm (258 nm)
	SOMO-3→LUMO+1	329 nm (309 nm)
	SOMO-1→LUMO+1	429 nm (431 nm)
	SOMO-LUMO	1.8 eV
(3)	SOMO-3→LUMO+3	269 nm (211 nm)
	SOMO-3→LUMO+2	274 nm (256 nm)
	SOMO-2→LUMO+2	308 nm (314 nm)
	SOMO-1→LUMO+1	429 nm (431 nm)
	SOMO-LUMO	1.9 eV
(4)	SOMO-3→LUMO+3	289 nm (255 nm)
	SOMO-2→LUMO+3	319 nm (309 nm)
	SOMO→LUMO+3	436 nm (431 nm)
	SOMO-LUMO	1.7 eV
(5)	SOMO-3→LUMO+2	257 nm (260 nm)
	SOMO-1→LUMO+2	329 nm (332 nm)
	SOMO-1→LUMO	479 nm (540 nm)
	SOMO→LUMO+1	588 nm (600 nm)
	SOMO-LUMO	1.8 eV

Values in parenthesis taken from [17].

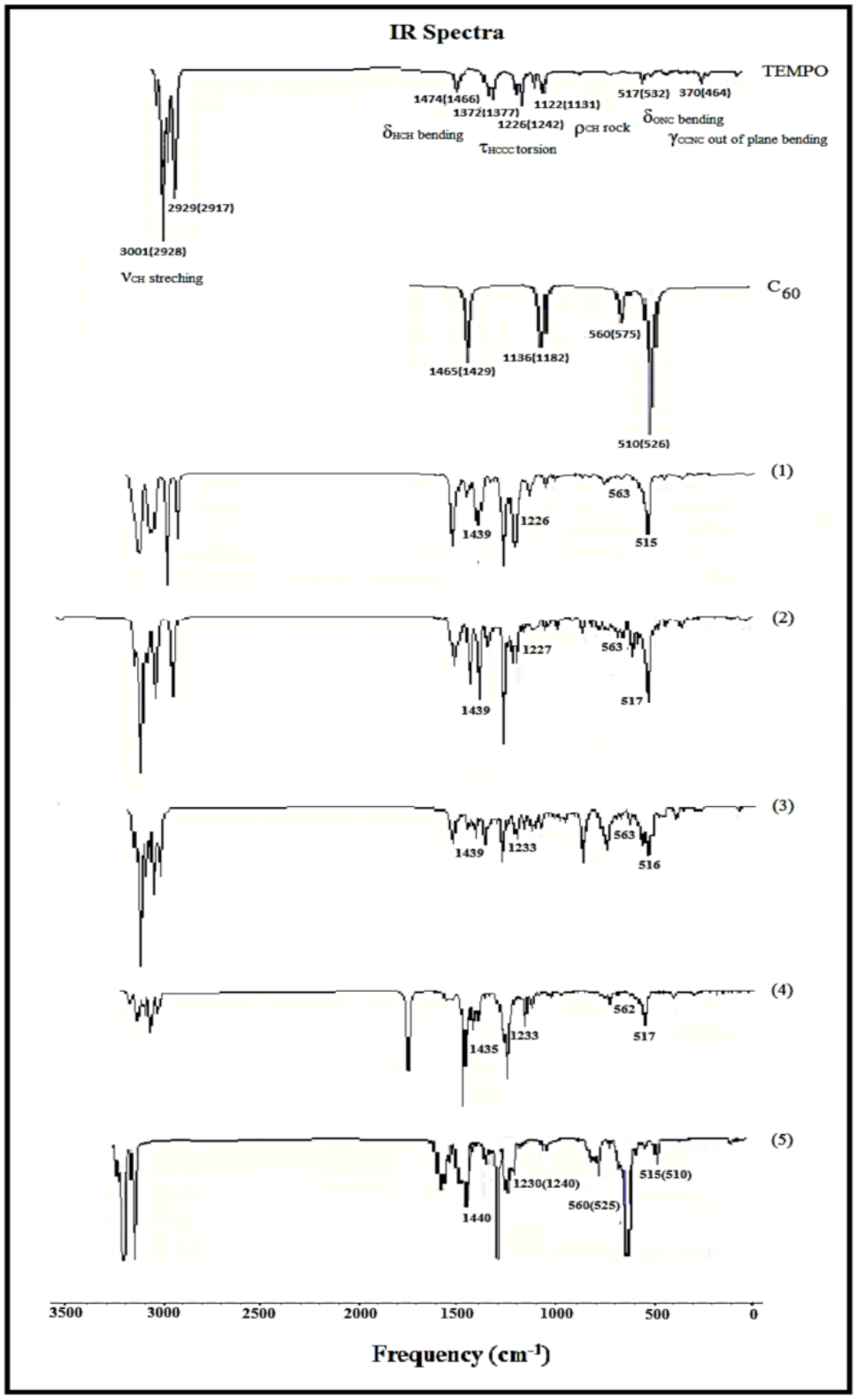

Fig. 6. The calculated IR absorption spectra of all the radical derivatives of the fullerene with together those belonged to the pure fullerene and 2,2,6,6-tetramethyl-piperidine-1-oxyl. The experimental values are given in parenthesis [17,19,20].

Isotropic hyperfine coupling constants

The calculated isotropic hyperfine coupling constants (hfcc's) and energies for the ground state optimized structures of all the radical products of C_{60}(TEMPO) are tabulated in Table 3. For comparison the experimental hfcc's of the ^{14}N nucleus are also given in the table [17]. Taking into account that the calculated results based on a single molecule may not match to the experimental one in which multiple interactions takes place, there is reasonable agreement between the calculated and experimental hfcc values. Also the isotropic hfcc's are very sensitive to the spin density at the nucleus position, so, are very difficult to compute in a quantitative agreement with the experimental data [21]. In Table 3 are also given the Mulliken atomic charges and spin densities of the N and O atoms and, the binding energies of the radicals for all the C_{60} (TEMPO) radical products. The Mulliken charges indicate a higher negative charge on the O atom than the N atom. Although the N and O atoms have close positive-spin densities, their nuclei have opposite-sign hfcc values. The binding energies of the labeled radicals in Table 3 shows the most tight-binding radical between the trapped radicals is (4) with a energy of -138.7 kcal.mol^{-1} while the most lost-binding radical is (5) with a energy of -102.6 kcal.mol^{-1}.

CONCLUSIONS

The TEMPO radical derivatives of the fullerene (C60) were theoretically investigated by spectroscopic techniques at the DFT(B3LYP)/6-31G(d) level of theory. It was concluded that a ring junction of the C_{60} moiety generally covalently linked to the piperidine ring of TEMPO, directly. The optimization characteristics of all the C_{60}(TEMPO) radical derivatives indicate them to have a 6-6 annulene structure while the C_{60}+TEMPO indicates a 6-6 cyclopropane structure. This was supported with the UV-Vis spectroscopic results. In the IR analysis it was seen that the C_{60} IR bands become weaker and, shift in the spectra of its TEMPO derivative products. Also the lowering of its symmetry gives rise to a number of bands assigned to the bending vibrations. The EPR analysis shows that

Table 3. The energy, isotropic hyperfine coupling constant (a), Mulliken spin density (ρ), atomic charge (Q), and radical's binding energy for the C60 (TEMPO) radical products calculated at DFT(B3LYP) 6-31 G(d) level. The experimental hyperfine coupling constants of the ^{14}N nucleus are given in parenthesis

	Energy (a.u.)	a_N (G)	a_O (G)	ρ_N	ρ_O	Q_N	Q_O	Binding energy of radical/BSSE corrected (kcal/mol)
TEMPO	-483.71403	11.26 (15.00)	-16.4	0.46	0.51	-0.03	-0.42	-
(1)	-2902.63036	12.83 (15.30)	-16.3	0.45	0.52	-0.03	-0.41	-130.7
(2)	-2863.33178	11.12 (15.15)	-16.4	0.46	0.52	-0.03	-0.42	-133.0
(3)	-2941.96262	13.94 (15.45)	-16.2	0.44	0.52	-0.05	-0.40	-120.2
(4)	-3016.00223	13.95 (15.38)	-16.2	0.44	0.52	-0.05	-0.40	-138.7
(5)	-2768.67189	11.09 (14.98)	-16.5	0.46	0.52	-0.03	-0.42	-102.6

Values in parenthesis taken from [17].

the hfcc's of the N and O nuclei for all the radical derivatives of C_{60}(TEMPO) are close but opposite-sign. But the N and O atoms have a nearly same positive spin density which can be induced by spin polarization.The some selected geometrical parameters with together cage width and cage length for the ground state optimized structures of all the radical adducts were listed, and the binding energies of the radicals were obtained. These labeled reagents seem to be applicable in studies on molecular systems, especially on bioorganic systems, containing fullerenes.

REFERENCES

[1] L.J. Berliner, Spin Labeling I: Theory and Applications, Academic Press, New York, 1976.

[2] L.J. Berliner, Spin Labeling II: Theory and Applications, Academic Press, New York, (979.

[3] T. Ishida, K. Shinozuka, M. Kubota, M. Ohashi and T. Nogami, J. Chem. Soc. Chem. Commun. 18 (1995) 1841.

[4] T. lshida, K. Shinozuka, T. Nogami, M. Kubota and M. Ohashi, Tetrahedron 52 (1996) 5103.

[5] M. J. Frisch, et al., Gaussian 09 Revision D.01, Gaussian Inc, Pittsburgh PA 2009.

[6] A. Frish, A.B. Nielsen and A.J. Holder, Gauss View User Manual, Gaussian Inc, Pittsburg PA 2001.

[7] S. Miertus, E. Scrocco and J. Tomasi, Chem. Phys. 55 (1981) 117.

[8] R. Cammi and J. Tomasi, J. Comput. Chem. 16 (1995) 1449.

[9] D.C. Young, Computional Chemistry: A Pratical Guide for Applying Techniques to Real-World Problems (Electronics), John Wiley & Sons Inc, New York, 2001.

[10] M.H. Jamroz, Vibrational Energy Distribution Analysis VEDA 4, Warsaw 2004.

[11] S.F. Boys and F. Bernardi, Mol. Phys. 100 (2002) 65.

[12] P.W. Stephens, L. Mihaly, P.L. Lee, R.L. Whetten, S.M. Huang, R. Kaner, F. Diederich and K. Holczer, Nature 351 (1991) 632.

[13] R.D. Johnson, G. Meijer and D.S. Bethune, J. Am. Chem. Soc. 112 (1990) 8983.

[14] G.L. Miessler, P.J. Fischer and D.A. Tarr, Inorganic Chemistry, Pearson, USA 2013.

[15] J. Laleve´e, X. Allonas and P. Jacques, J. Mol. Struct: Theochem 767 (2006) 143.

[16] R.C. Haddon, L.E. Brus and K. Raghavachari, Chem. Physic Lett. 125 (1986) 459.

[17] F. Arena, F. Bullo, F. Conti, C. Corvaja, M. Maggini, M. Prato and G. Scorrano, J. Am. Chem. Soc. 119 (1997) 789.

[18] K. Fukui, Scienc. 218 (1982) 747.

[19] V.N. Ivanova, V.A. Nadolinnyi, I.A. Grigor'ev and E. Rejerse, Phys. Solid State 44 (2002) 560.

[20] Spectral Database for Organic Compounds Web Page, National Institute of Advanced Industrial Science and Technology (AIST), Japan 2001.

[21] D. Feller and E.R. Davidson, J. Chem. Phys. 80 (1984) 1006.